Supplementary information

Current Blockades of Proteins Inside Nanopores for Real-Time Metabolome Analysis

Sarah Zernia[†], Nieck Jordy van der Heide[†], Nicole Stéphanie Galenkamp[†], Giorgos Gouridis[‡], Giovanni Maglia[†,*]

[†] Groningen Biomolecular Sciences & Biotechnology Institute, University of Groningen, Nijenborgh 7, 9747 AG Groningen, The Netherlands

[‡] Rega Institute for Medical Research, Laboratory of Molecular Bacteriology, KU Leuven, Herestraat 49 – box 1037, 3000 Leuven, Belgium

Protein sequences of the used adaptor proteins

Periplasmid signal sequences are underlined with dashed lines, His-tag with straight lines

Substrate binding protein 1 (SBD1) of GlnPQ from *Lactococcus lactis*:
MKKLFFALAMMLATVTAFLVAPSVKAETTVKIASDSSYAPFEFQNGQKKWVGIDVDIMQEVAKIN
DWKLEMSYPGFDAALQNLKAGQVDGIIAGMTITDERKETFDFSNPYYTSALTIATTKDSKLSDYS
DLKGKAVGAKNGTAAQTWLQENQKKYGYTIKTYSDGVHMFAALSSGNIAGAMDEVPVISYAMK
QGQDLAMNFPSISLPGGYGFAVMKGKNSTLVDGFNKALAEMKSNGDYDKILKKYGITAGSSHH
HHHH

Nicotinamidase (Pnc1p) from *Saccharomyces cerevisiae*:
MKTLIVVDMQNDFISPLGSLTVPKGEELINPISDLMQDADRDWHRIVVTRDWHPSRHISFAKNHK
DKEPYSTYTYHSPRPGDDSTQEGILWPVHCVKNTWGSQLVDQIMDQVVTKHIKIVDKGFLTDR
EYYSAFHDIWNFHKTDMNKYLEKHHTDEVYIVGVALEYCVKATAISAAELGYKTTVLLDYTRPIS
DDPEVINKVKEELKAHNINVVDKLEHHHHHH

Nicotinamidase dipole mutant (Pnc1p_dipole) from *Saccharomyces cerevisiae*:
MKTLIVVDMQNDFISPLGSLTVPKGEELINPISDLMQDADRDWHRIVVTRDWHPSRHISFAKNHK
DKEPYSTYTYHSPRPGKKSTQEGILWPVHCVKNTWGSQLVDQIMDQVVTKHIKIVDKGFLTDRE
YYSAFHDIWNFHKTDMNKYLEKHHTDEVYIVGVALEYCVKATAISAAELGYKTTVLLDYTRPISD
DPEVINKVKEELKAHNINVVDE

Substrate binding protein 2 (SBD 2) of GlnPQ from *Lactococcus lactis*:
MHHHHHHHHHHGENLYFQGMATPKKDVYTIASDNSFAPFEFQNDDKQFTGIDVDLLNAIAKNQ
GFKLKWNFIGFQAAVDSVQSGHADGMMSGMSITDARKQVFDYGSPYYSSNLTIATSSTDDSIK
SWKDLKGKTLGAKNGTASFDYLNAHAKEYGYTVKTFTDATTMYSSLNNGSINALMDDEPVIKYA
IKQGQKFATPIKPIPDGQYGFAVKKGSNPELIEMFNNGLANLRANGEYDKIIDKYLESDA

Vitamin B12 binding protein (BtuF) of BtuCDF from *Escherichia coli*:
MKYLLPTAAAGLLLLAAQPAMAMAAPRVITLSPANTELAFAAGITPVGVSSYSDYPPQAQKIEQV
STWQGMNLERIVALKPDLVIAWRGGNAERQVDQLASLGIKVMWVDATSIEQIANALRQLAPWS
PQPDKAEQAAQSLLDQYAQLKAQYADKPKKRVFLQFGINPPFTSGKESIQNQVLEVCGGENIFK
DSRVPWPQVSREQVLARSPQAIVITGGPDQIPKIKQYWGEQLKIPVIPLTSDWFERASPRIILAAQ
QLCNALSQVDLEHHHHHH

Hoefavidin-short from *Hoeflea phototrophica*:
MFADDHAMSPDMKLLAGASNWVNQSGSVAQFVFTPSPTQPQTYEVSGNYINNAQGTGCKGT
PYPLSGAYYSGNQIISFSVVWSNASANCQSATGWTGYFDFSGSQAVLKTDWNLAFYSGSTPAI
QQGQDDFMQSVLEHHHHHH

Myo-Inositol binding protein (IbpA) of latP-latA ATP binding cassette from *Caulobacter vibrioides*:
MANKKVLTLSAVMASMLFGAAAHAGLVPRGSHMEVVVSFNDLSQPFFVAMRRELEDEAAKLG
VKVQVLDAQNNSSKQISDLQAAAVQGAKVVIVAPTDSKALAGAADDLVEQGVAVISVDRNIAGG
KTAVPHVGADNVAGGRAMADWVVKTYPAGARVVVITNDPGSSSSIERVKGVHDGLAAGGPAF
KIVTEQTANSKRDQALTVTQNILTSMRDTPPDVILCLNDDMAMGALEAVRAAGLDSAKVKVIGFD
AIPEALARIKAGEMVATVEQNPGLQIRTALRQAVDKIKSGAALKSVSLKPVLITSGNLTEASRIGE
MGSSHHHHHH

Glucose-/ Galactose binding protein (GGBP) from *Escherichia coli*:
MANKKVITLSAVMASMLFGAAAHAADTRIGVTIYKYDDNFMSVVRKAIEQDAKAAPDVQLLMND
SQNDQSKQNDQIDVLLAKGVKALAINLVDPAAAGTVIEKARGQNVPVVFFNKEPSRKALDSYDK

AYYVGTDSKESGIIQGDLIAKHWAANQGWDLNKDGQIQFVLLKGEPGHPDAEARTTYVIKELND
KGIKTEQLQLDTAMWDTAQAKDKMDAWLSGPNANKIEVVIANNDAMAMGAVEALKAHNKSSIP
VFGVDALPEALALVKSGALAGTVLNDANNQAKATFDLAKNLADGKGAADGTNWKIDNKVVRVP
YVGVDKDNLAEFSKKGSSHHHHHH

Sialic acid binding protein (SiaP) of TRAP transporter from *Pasteurella multocida*:
MGKFKKLLLASLCLGVSASVFAADYDLKFGMVAGPSSNEYKAVEFFAKEVKEKSNGKIDVAIFP
SSQLGDDRVMIKQLKDGALDFTLGESARFQIYFPEAEVFALPYMIPNFETSKKALLDTKFGQGLL
KKIDKELNVQVLSVAYNGTRQTTSNRAINSIEDMKGLKLRVPNAATNLAYAKYVGAAPTPMAFS
EVYLALQTNSVDGQENPLPTIQAQKFYEVQKYLALTNHILNDQLYLISNDTLADLPEDLQKVVKD
AAAKAAEYHTKLFVDGENSLVEFFKSQGVTVTQPDLKPFKAALTPYYDEYLKKNGEVGKMAIEEI
SNLAKLGSSHHHHHH

Thiamine binding protein (TbpA) of an ABC transporter from *Escherichia coli*:
MGLKKCLPLLLLCTAPVFAMGSSHHHHHHSSGLVPRGSHMKPVLTVYTYDSFAADWGPGPVV
KKAFEADCNCELKLVALEDGVSLLNRLRMEGKNSKADVVLGLDNNLLDAASKTGLFAKSGVAA
DAVNVPGGWNNDTFVPFDYGYFAFVYDKNKLKNPPQSLKELVESDQNWRVIYQDPRTSTPGL
GLLLWMQKVYGDDAPQAWQKLAKKTVTVTKGWSEAYGLFLKGESDLVLSYTTSPAYHILEEKK
DNYAAANFSEGHYLQVEVAARTAASKQPELAQKFLQFMVSPAFQNAIPTGNWMYPVANVTLPA
GFEKLTKPATTLEFTPAEVAAQRQAWISEWQRAVSR

Leucine binding protein (LBP) of an ABC transporter from *Escherichia coli*:
MGKRNAKTIIAGMIALAISHTAMADDIKVAVVGAMSGPIAQWGDMEFNGARQAIKDINAKGGIKG
DKLVGVEYDDACDPKQAVAVANKIVNDGIKYVIGHLCSSSTQPASDIYEDEGILMISPGATNPELT
QRGYQHIMRTAGLDSSQGPTAAKYILETVKPQRIAIIHDKQQYGEGLARSVQDGLKAANANVVF
FDGITAGEKDFSALIARLKKENIDFVYYGGYYPEMGQMLRQARSVGLKTQFMGPEGVGNASLS
NIAGDAAEGMLVTMPKRYDQDPANQGIVDALKADKKDPSGPYVWITYAAVQSLATALERTGSD
EPLALVKDLKANGANTVIGPLNWDEKGDLKGFDFGVFQWHADGSSTAAKGSSHHHHHH

Spermidine binding protein (SpuE) of SpuDEFGH from *Escherichia coli*:
MQHSIGKTLLVAALATAIAGPVQAEKKSLHIYNWTDYIAPTTLKDFTKESGIDVSYDVFDSNETLE
GKLVSGHSGYDIVVPSNNFLGKQIQAGAFQKLDKSKLPNWKNLDPALLKQLEVSDPGNQYAVP
YLWGTNGIGYNVAKVKEVLGDQPIDSWAILFEPENMKKLAKCGVAFMDSGDEMLPAALNYLGL
DPNTHDPKDYKKAEEVLTKVRPYVSYFHSSKYISDLANGNICVAFGYSGDVFQAAARAEEAGK
GIDIQYVIPKEGANLWFDLMAIPADAKAADNAYAFIDYLLRPEVIAKVSDYVGYANAIPGARPLMD
KSVSDSEEVYPPQAVLDKLYVSAVLPAKVLRLQTRTWTRIKTGKLEHHHHHH

Putrescine binding protein (SpuD) of SpuDEFGH from *Escherichia coli*:
MGMKRFGKTLLALTLAGSVAGMAQAADNKVLHVYNWSDYIAPDTLEKFTKETGIKVVYDVYDS
NEVLEAKLLAGKSGYDVVVPSNSFLAKQIKAGVYQKLDKSKLPNWKNLNKDLMHTLEVSDPGN
EHAIPYMWGTIGIGYNPDKVKAAFGDNAPVDSWDLVFKPENIQKLKQCGVSFLDSPTEILPAALH
YLGYKPDTDNPKELKAAEELFLKIRPYVTYFHSSKYISDLANGNICVAIGYSGDIYQAKSRAEEAK
NKVTVKYNIPKEGAGSFFDMVAIPKDAENTEGALAFVNFLMKPEIMAEITDVVQFPNGNAAATPL
VSEAIRNDPGIYPSEEVMKKLYTFPDLPAKTQRAMTRSWTKIKSGKGSSHHHHHH

Maltose or maltodextrin binding protein (MBP) of an ABC transporter from *Escherichia coli*:
MKIEEGKLVIWINGDKGYNGLAEVGKKFEKDTGIKVTVEHPDKLEEKFPQVAATGDGPDIIFWAH
DRFGGYAQSGLLAEITPDKAFQDKLYPFTWDAVRYNGKLIAYPIAVEALSLIYNKDLLPNPPKTW
EEIPALDKELKAKGKSALMFNLQEPYFTWPLIAADGGYAFKYENGKYDIKDVGVDNAGAKAGLT
FLVDLIKNKHMNADTDYSIAEAAFNKGETAMTINGPWAWSNIDTSKVNYGVTVLPTFKGQPSKP

FVGVLSAGINAASPNKELAKEFLENYLLTDEGLEAVNKDKPLGAVALKSYEEELAKDPRIAATME
NAQKGEIMPNIPQMSAFWYAVRTAVINAASGRQTVDEALKDAQTRITKLE<u>HHHHHH</u>

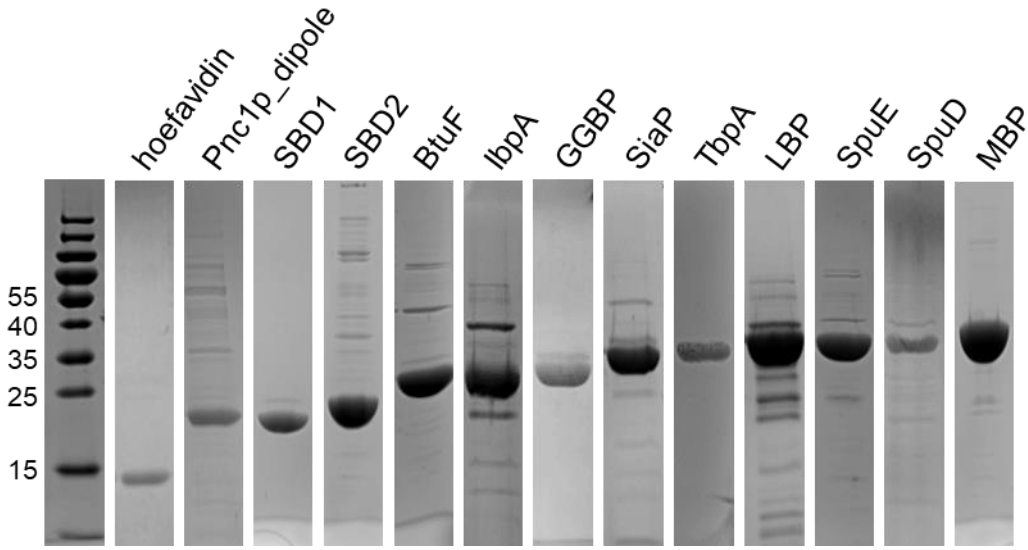

Figure S1. SDS PAGE of purified proteins for this study. 12 % SDS gel, ProBlue stain, ladder: PageRuler prestained. Hoefavidin monomer: 15.4 kDa; Pnc1p_dipole: 25.0 kDa; SBD1: 25.5 kDa; SBD2: 27.8 kDa; BtuF: 28 kDa; IbpA: 31.8 kDa; GGBP: 34.3 kDa; SiaP: 35.2 kDa; TbpA: 36.5 kDa; LBP: 38 kDa; SpuE: 38.8 kDa; SpuD: 39.2 kDa; MBP: 41.9 kDa.

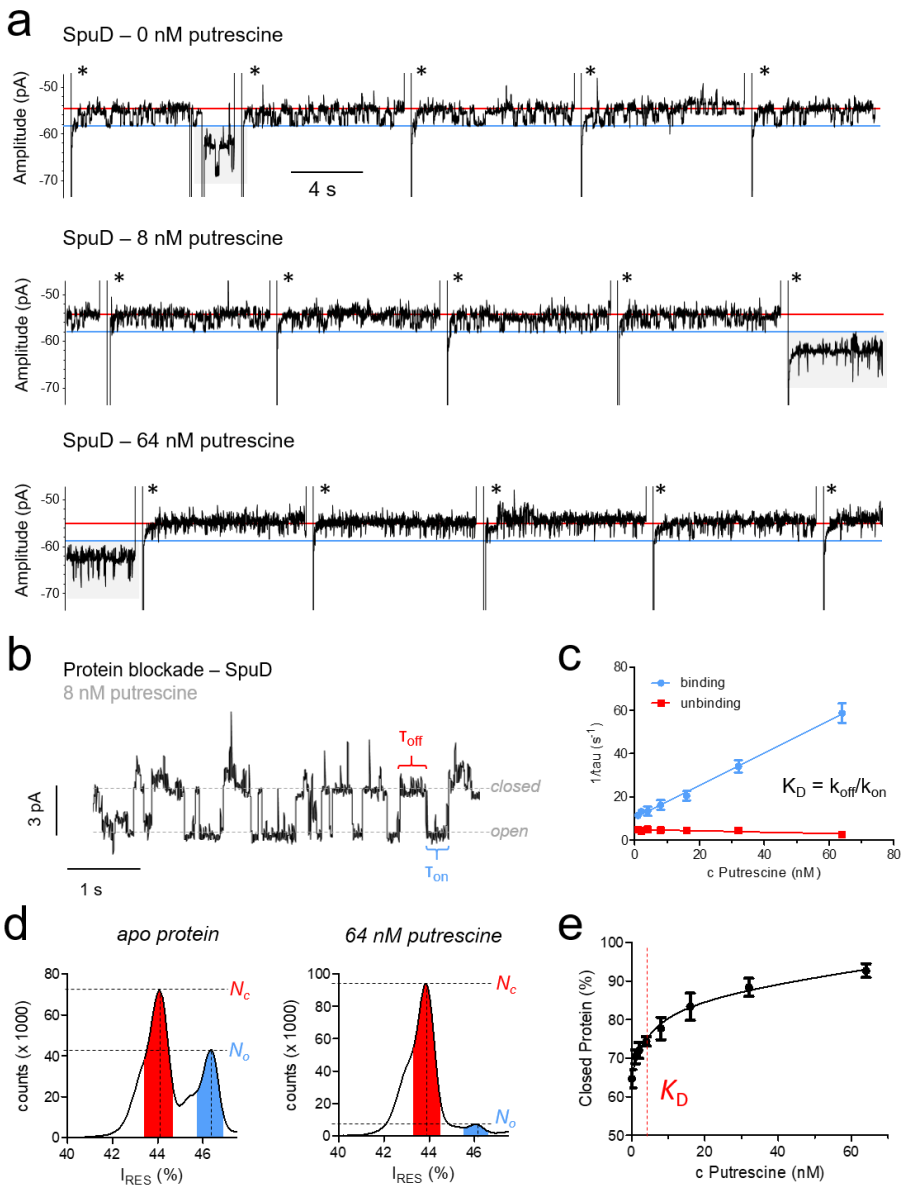

Figure S2. Protein blockades and binding curve of putrescine binding protein SpuD. **(a)** Typical current blockade of SpuD (74 nM) in the absence and presence of putrescine (*cis*). The current corresponding to the open protein state is labelled in blue, the closed protein state in red. Asterisks label single protein molecules entering/exiting the nanopore. Grey shaded blockades were excluded from analysis. **(b)** Zoom-in of the protein blockade. **(c)** Association and dissociation rates are plotted against the ligand concentration. **(d)** All-point histograms of a typical protein blockade in *apo* state and after addition of 64 nM putrescine. The peak representing the open state is labelled in blue, the closed state in red. The number of counts at the maximum of each peak (NC and No, for the peaks corresponding to the closed and the open configuration, respectively) was used for determination of the percentage of the closed protein [Closed Protein (%) = $N_C/(N_O+N_C)$]. **(e)** Percentage of closed protein as a dependence of the putrescine concentration. For K_D determination, the data points were fitted to a binding isotherm. Measurements were performed in 15 mM Tris, 150 mM NaCl, pH 7.5 applying -80 mV to the *trans* side and sampling at 10 kHz with a 2 kHz Bessel filter. For figure preparation, all traces were additionally filtered with a 100 Hz Gaussian filter. Protein and ligand were added to the *cis* side of the pore. The error bars represent the standard error of the mean for at least three experiments.

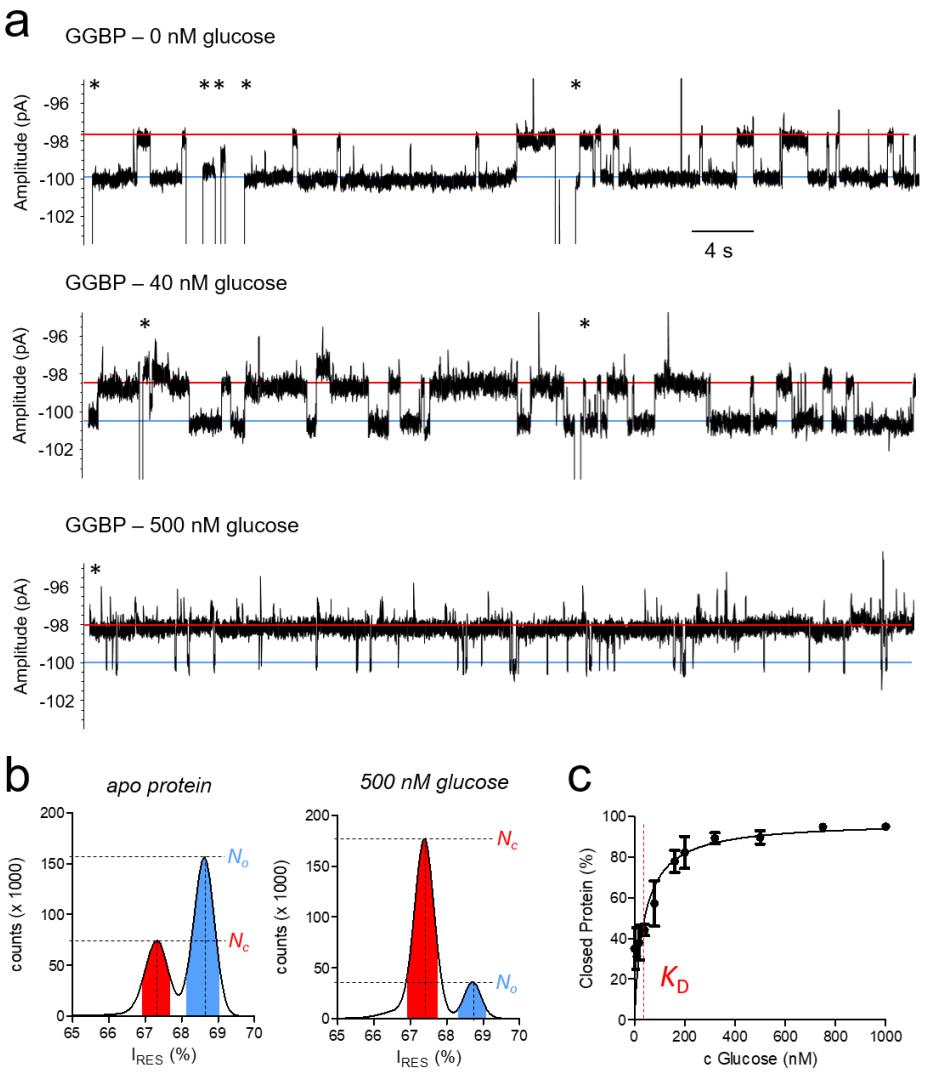

Figure S3. Protein blockades and binding curve of glucose binding protein GGBP. **(a)** Typical current blockade of GGBP (50 nM) in the absence and presence of glucose (*cis*). The current corresponding to the open protein state is labelled in blue, the closed protein state in red. Asterisks label single protein molecules entering/exiting the nanopore. **(b)** All-point histograms based on the I_{RES} (I_B/I_O) of the protein blockade in *apo* state and after addition of 500 nM glucose. The peak representing the open state is labelled in blue, the closed state in red. The number of counts at the maximum of each peak (NC and No, for the peaks corresponding to the closed and the open configuration, respectively) was used for determination of the percentage of the closed protein [Closed Protein (%) = $N_C/(N_O+N_C)$]. **(c)** Percentage of closed protein as a dependence of the glucose concentration. For K_D determination, the data points were fitted to a binding isotherm. Measurements were performed in 15 mM Tris, 150 mM NaCl, pH 7.5 applying -90 mV to the *trans* side and sampling at 10 kHz with a 2 kHz Bessel filter. For figure preparation, all traces were additionally filtered with a 100 Hz Gaussian filter. Protein and ligand were added to the *cis* side of the pore. The error bars represent the standard error of the mean for at least three experiments.

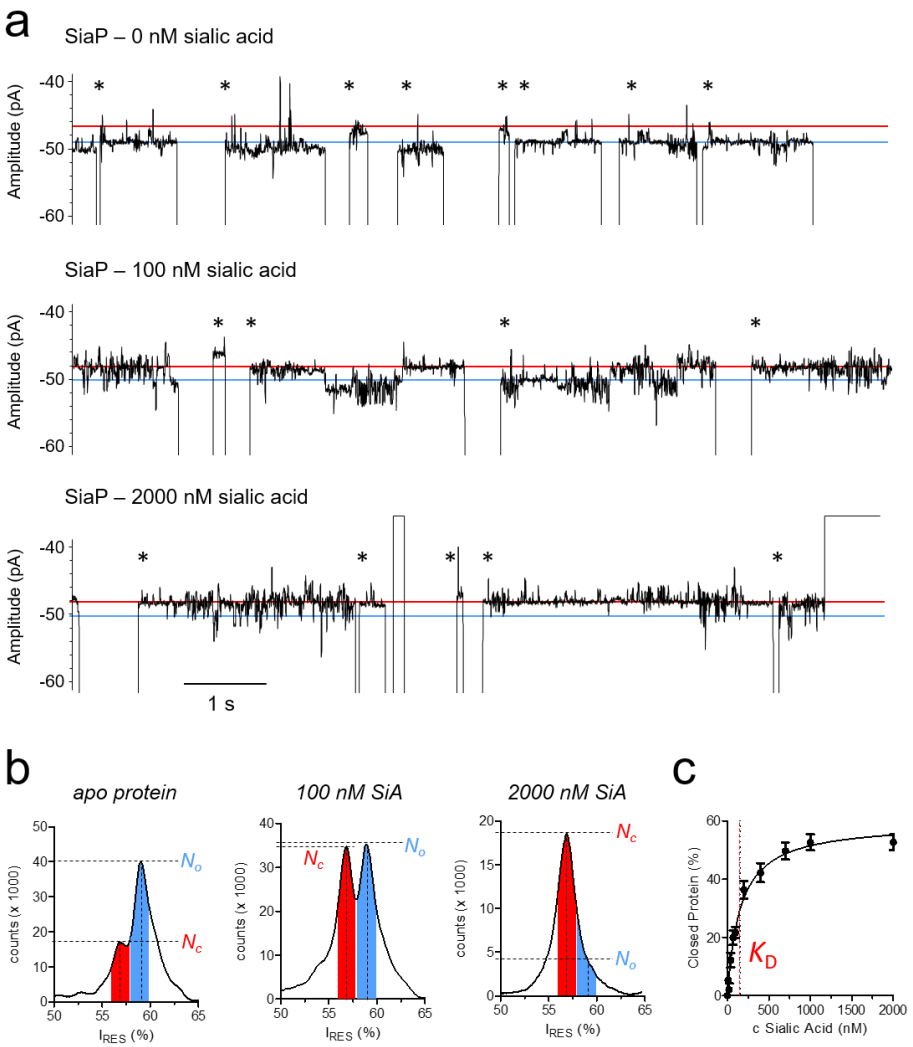

Figure S4. Protein blockades and binding curve of sialic acid binding protein SiaP. **(a)** Typical current blockade of SiaP (352 nM) in the absence and presence of sialic acid (*cis*). The current corresponding to the open protein state is labelled in blue, the closed protein state in red. Asterisks label single protein molecules entering/exiting the nanopore. **(b)** All-point histograms based on the I_{RES} (I_B/I_O) of the protein blockade in *apo* state and after addition of 100 and 2000 nM sialic acid (SiA). The peak representing the open state is labelled in blue, the closed state in red. The number of counts at the maximum of each peak (NC and No, for the peaks corresponding to the closed and the open configuration, respectively) was used for determination of the percentage of the closed protein [Closed Protein (%) = $N_C/(N_O+N_C)$]. **(c)** Percentage of closed protein as a dependence of the sialic acid concentration. For K_D determination, the data points were fitted to a binding isotherm. Measurements were performed in 15 mM Tris, 150 mM NaCl, pH 7.5 applying -90 mV to the *trans* side and sampling at 10 kHz with a 2 kHz Bessel filter. For figure preparation, all traces were additionally filtered with a 100 Hz Gaussian filter. Protein and ligand were added to the *cis* side of the pore. The error bars represent the standard error of the mean for at least three experiments.

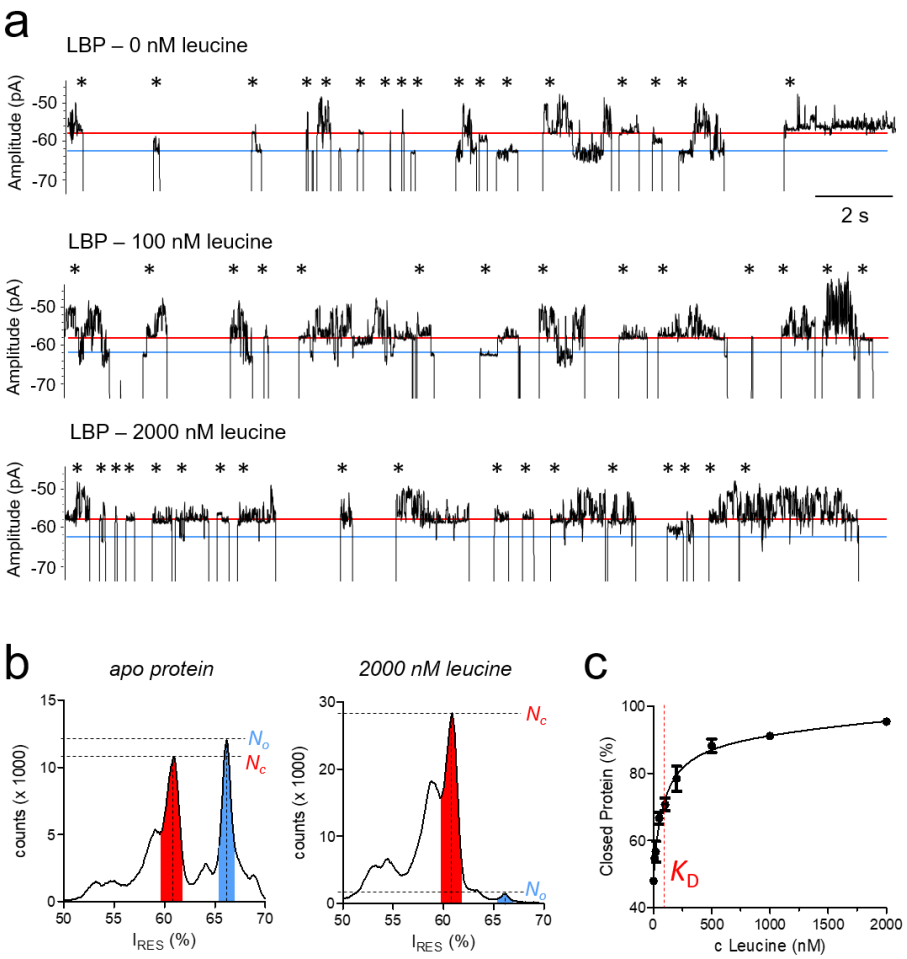

Figure S5. Protein blockades and binding curve of leucine binding protein LBP. **(a)** Typical current blockade of LBP (272 nM) in the absence and presence of leucine (*cis*). The current corresponding to the open protein state is labelled in blue, the closed protein state in red. Asterisks label single protein molecules entering/exiting the nanopore. **(b)** All-point histograms based on the I_{RES} (I_B/I_O) of the protein blockade in *apo* state and after addition of 2000 nM leucine. The peak representing the open state is labelled in blue, the closed state in red. The number of counts at the maximum of each peak (NC and No, for the peaks corresponding to the closed and the open configuration, respectively) was used for determination of the percentage of the closed protein [Closed Protein (%) = $N_C/(N_O+N_C)$]. **(c)** Percentage of closed protein as a dependence of the leucine concentration. For K_D determination, the data points were fitted to a binding isotherm. Measurements were performed in 15 mM Tris, 150 mM NaCl, pH 7.5 applying -60 mV to the *trans* side and sampling at 10 kHz with a 2 kHz Bessel filter. For figure preparation, all traces were additionally filtered with a 100 Hz Gaussian filter. Protein and ligand were added to the *cis* side of the pore. The error bars represent the standard error of the mean for at least three experiments.

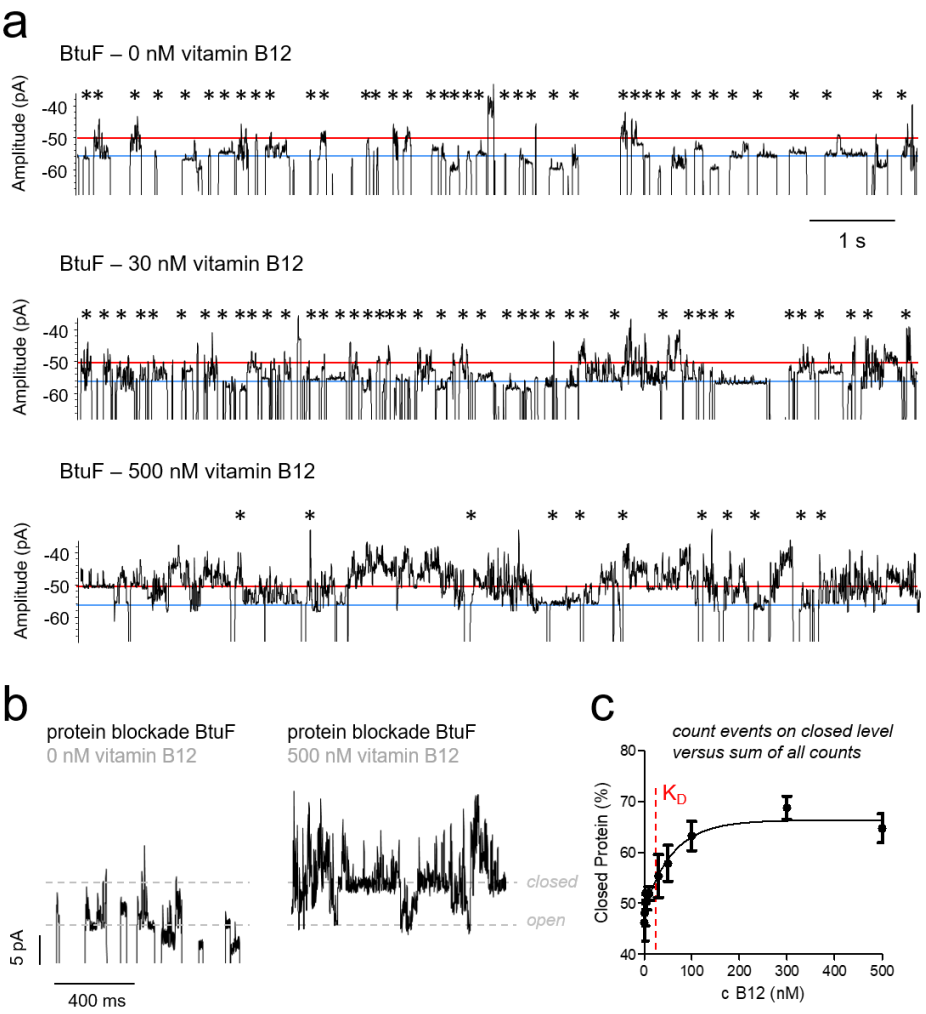

Figure S6. Protein blockades and binding curve of CN-cobalamine (vitamin B12) binding protein BtuF. **(a)** Typical current blockade of BtuF (34 nM) in the absence and presence of vitamin B12 (*cis*). The current corresponding to the open protein state is labelled in blue, the closed protein state in red. Asterisks label single protein molecules entering/exiting the nanopore. **(b)** Zoom-in to the protein blockade visualizing the increase of events at the closed level. The number of events on closed level were counted and divided by the number of all counted events resulting in an amount of closed protein. **(c)** Percentage of closed protein as a dependence of the vitamin B12 concentration. For K_D determination, the data points were fitted to a binding isotherm. Measurements were performed in 15 mM Tris, 150 mM NaCl, pH 7.5 applying -55 mV to the *trans* side and sampling at 10 kHz with a 2 kHz Bessel filter. For figure preparation, all traces were additionally filtered with a 100 Hz Gaussian filter. Protein and ligand were added to the *cis* side of the pore. The error bars represent the standard error of the mean for at least three experiments.

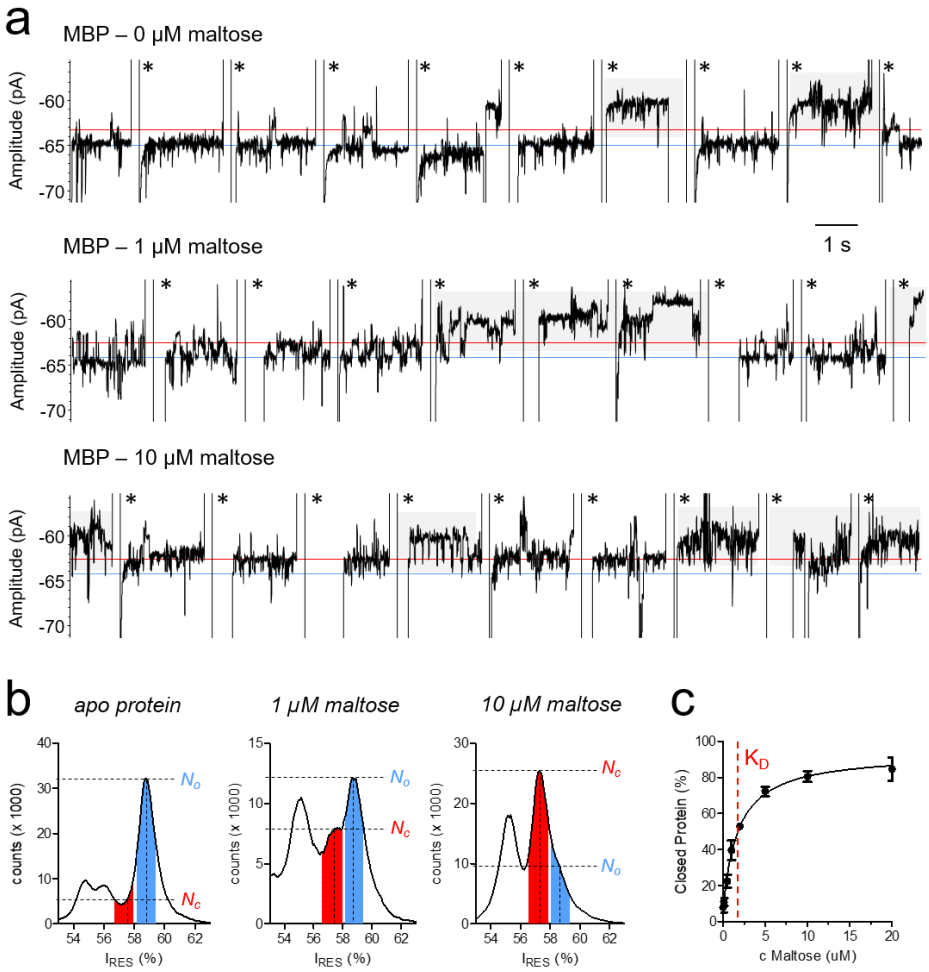

Figure S7. Protein blockades and binding curve of maltose binding protein MBP. **(a)** Typical current blockade of MBP (48 µM) in the absence and presence of maltose (*cis*). The current corresponding to the open protein state is labelled in blue, the closed protein state in red. Asterisks label single protein molecules entering/exiting the nanopore. Grey areas represent alternative blockades. **(b)** All-point histograms based on the I_{RES} (I_B/I_O) of the protein blockade in *apo* state and after addition of 1 µM and 10 µM maltose. The peak representing the open state is labelled in blue, the closed state in red. The number of counts at the maximum of each peak (NC and No, for the peaks corresponding to the closed and the open configuration, respectively) was used for determination of the percentage of the closed protein [Closed Protein (%) = $N_C/(N_O+N_C)$]. **(c)** Percentage of closed protein as a dependence of the maltose concentration. For K_D determination, the data points were fitted to a binding isotherm. Measurements were performed in 15 mM Tris, 150 mM NaCl, pH 7.5 applying -70 mV to the *trans* side and sampling at 10 kHz with a 2 kHz Bessel filter. For figure preparation, all traces were additionally filtered with a 100 Hz Gaussian filter. Protein and ligand were added to the *cis* side of the pore. The error bars represent the standard error of the mean for at least three experiments.

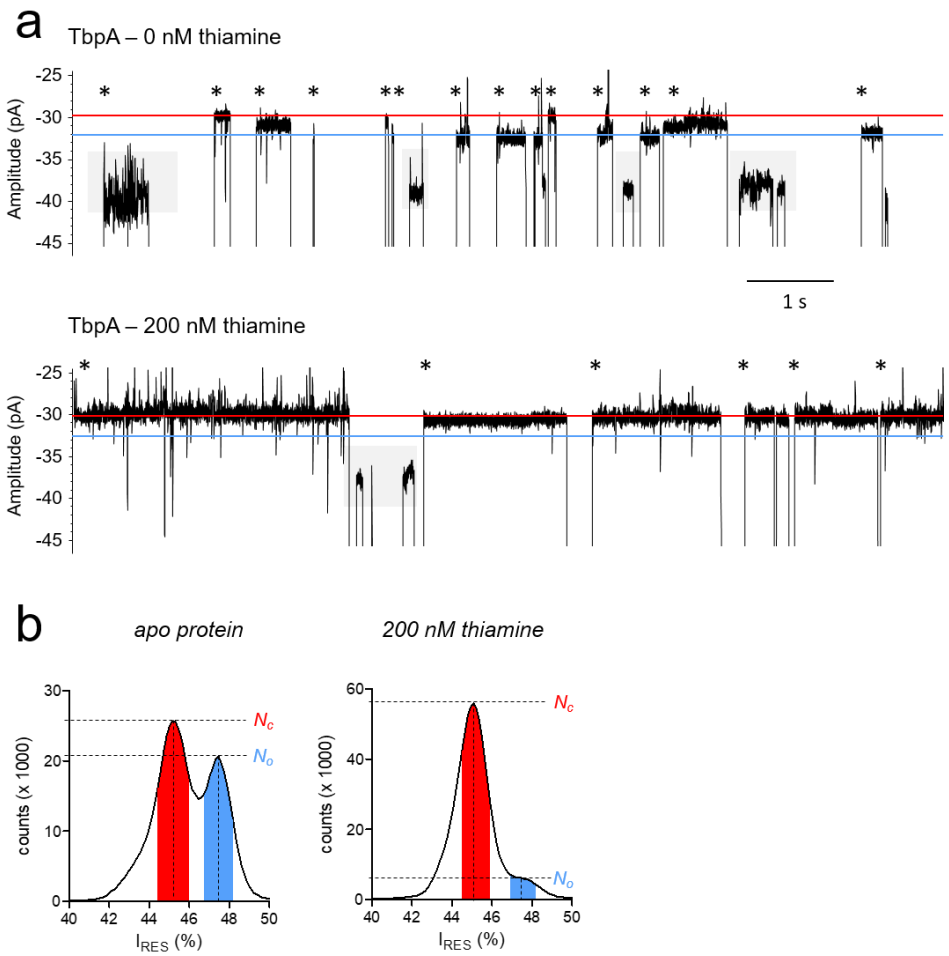

Figure S8. Protein blockades of thiamine binding protein TbpA. **(a)** Typical current blockade of TbpA (135 nM) in the absence and presence of thiamine (*cis*). The current corresponding to the open protein state is labelled in blue, the closed protein state in red. Asterisks label single protein molecules entering/exiting the nanopore. Grey areas represent alternative blockades. **(b)** All-point histograms based on the I_{RES} (I_B/I_O) of the protein blockade in *apo* state and after addition of 200 nM thiamine. The peak representing the open state is labelled in blue, the closed state in red. The number of counts at the maximum of each peak (NC and No, for the peaks corresponding to the closed and the open configuration, respectively) was used for determination of the percentage of the closed protein [Closed Protein (%) = $N_C/(N_O+N_C)$]. Measurements were performed in 15 mM Tris, 150 mM NaCl, pH 7.5 applying -35 mV to the *trans* side and sampling at 10 kHz with a 2 kHz Bessel filter. For figure preparation, all traces were additionally filtered with a 100 Hz Gaussian filter. Protein and ligand were added to the *cis* side of the pore.

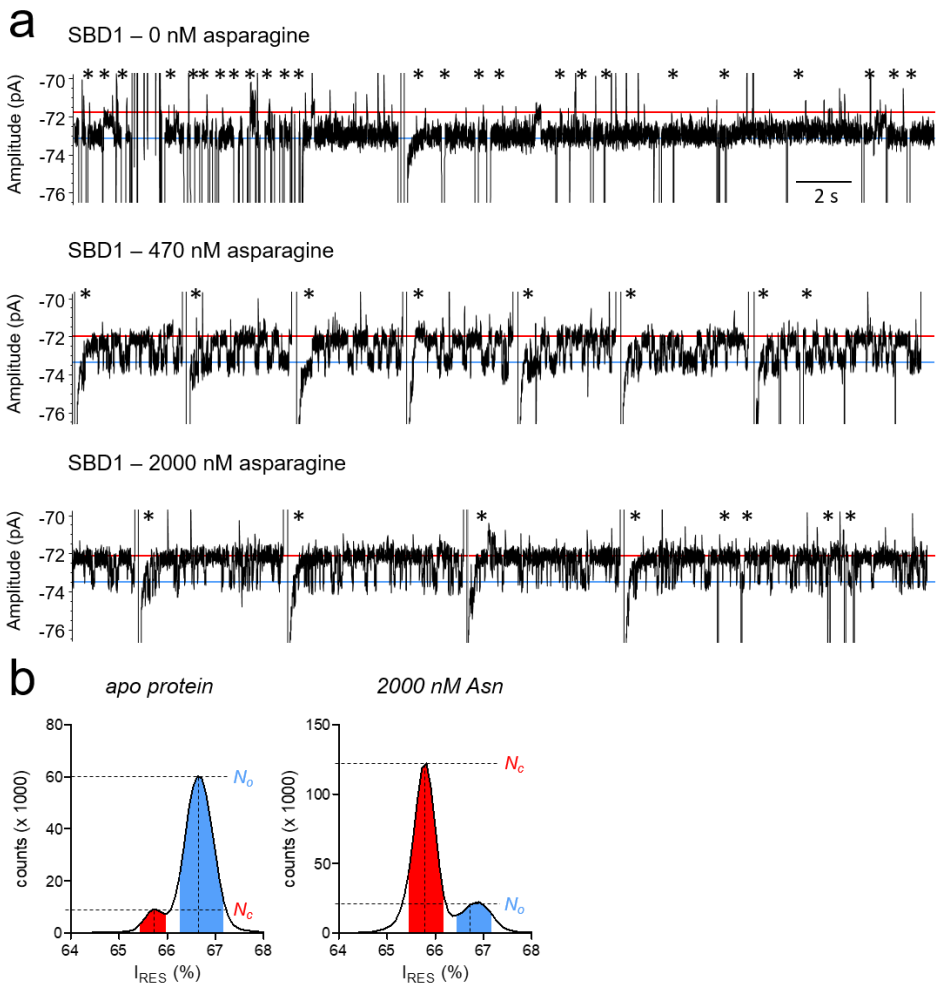

Figure S9. Protein blockades of asparagine binding protein SBD1. **(a)** Typical current blockade of SBD1 (74 nM) in the absence and presence of asparagine (*cis*). The current corresponding to the open protein state is labelled in blue, the closed protein state in red. Asterisks label single protein molecules entering/exiting the nanopore. **(b)** All-point histograms based on the I_{RES} (I_B/I_O) of the protein blockade in *apo* state and after addition of 2000 nM asparagine. The peak representing the open state is labelled in blue, the closed state in red. The number of counts at the maximum of each peak (NC and No, for the peaks corresponding to the closed and the open configuration, respectively) was used for determination of the percentage of the closed protein [Closed Protein (%) = $N_C/(N_O+N_C)$]. Measurements were performed in 15 mM Tris, 150 mM NaCl, pH 7.5 applying -70 mV to the *trans* side and sampling at 10 kHz with a 2 kHz Bessel filter. For figure preparation, all traces were additionally filtered with a 100 Hz Gaussian filter. Protein and ligand were added to the *cis* side of the pore. K_D was taken from literature (see Table 1).

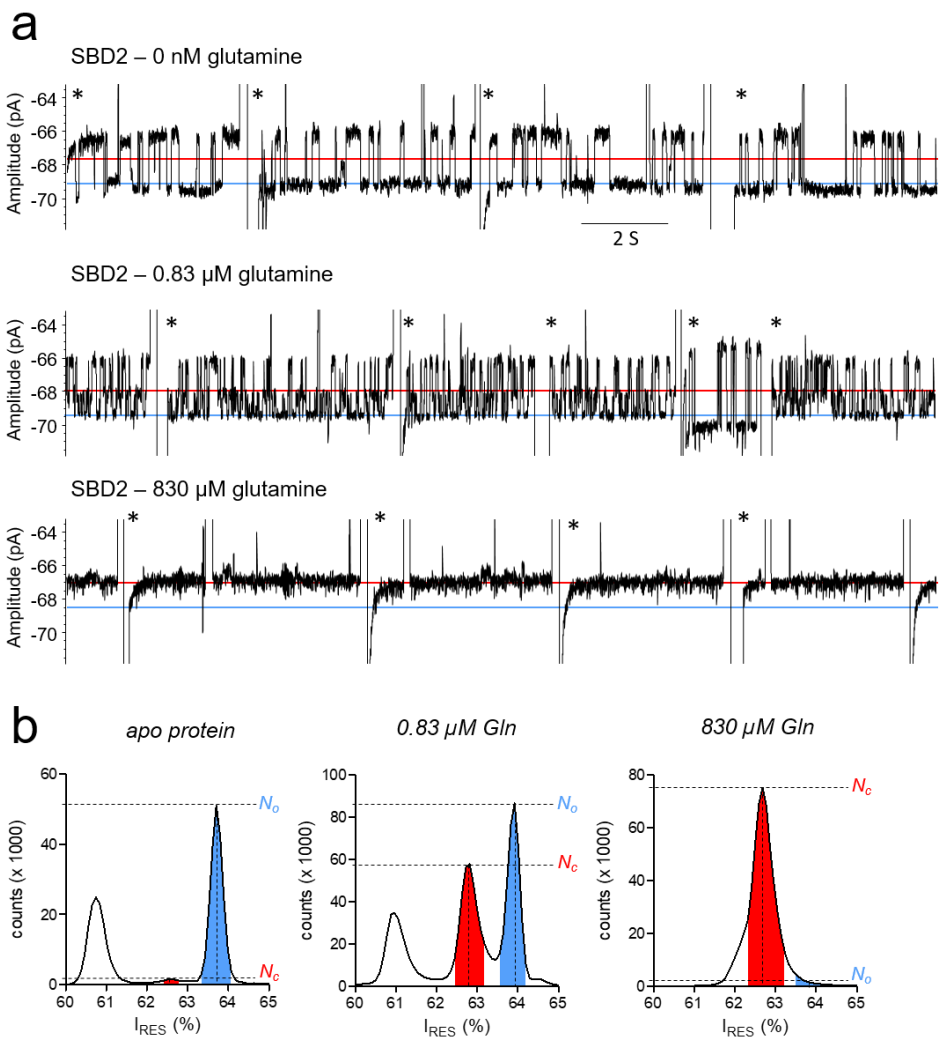

Figure S10. Protein blockades of glutamine binding protein SBD2. **(a)** Typical current blockade of SBD2 (72 nM) in the absence and presence of glutamine (*cis*). The current corresponding to the open protein state is labelled in blue, the closed protein state in red. Asterisks label single protein molecules entering/exiting the nanopore. **(b)** All-point histograms based on the I_{RES} (I_B/I_O) of the protein blockade in *apo* state and after addition of 0.83 µM or 830 µM glutamine. The peak representing the open state is labelled in blue, the closed state in red. The number of counts at the maximum of each peak (NC and No, for the peaks corresponding to the closed and the open configuration, respectively) was used for determination of the percentage of the closed protein [Closed Protein (%) = $N_C/(N_O+N_C)$]. Measurements were performed in 15 mM Tris, 150 mM NaCl, pH 7.5 applying -70 mV to the *trans* side and sampling at 10 kHz with a 2 kHz Bessel filter. For figure preparation, all traces were additionally filtered with a 100 Hz Gaussian filter. Protein and ligand were added to the *cis* side of the pore. K_D was taken from literature (see Table 1).

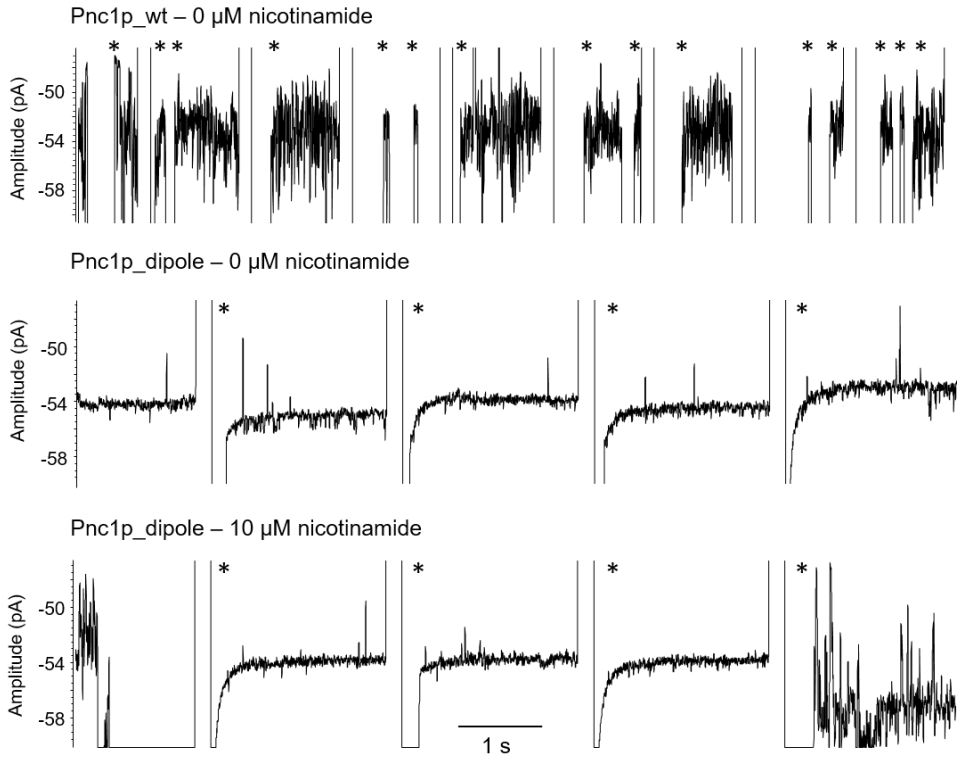

Figure S11. Protein blockades and binding curve of nicotinamidase Pnc1p. The protein was mutated at positions D82K, D83K, K216E to silence the signal resulting in the construct Pnc1p_dipole. Asterisks label single protein molecules entering/exiting the nanopore. An open and closed protein signal could not be identified. Measurement was performed in 15 mM Tris, 150 mM NaCl, pH 7.5 applying -60 mV to the *trans* side and sampling at 10 kHz with a 2 kHz Bessel filter. For figure preparation, all traces were additionally filtered with a 100 Hz Gaussian filter. Protein and ligand were added to the *cis* side of the pore.

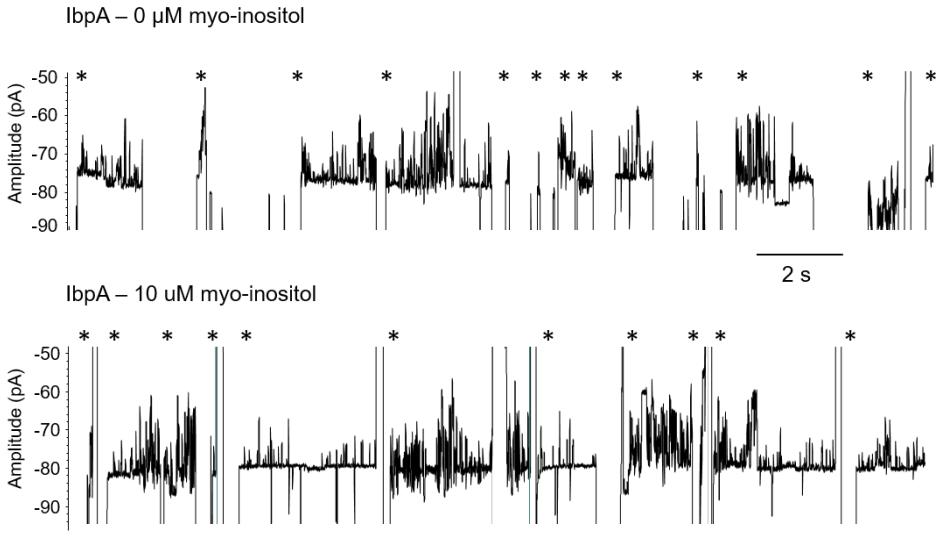

Figure S12. Protein blockades and binding curve of myo-inositol binding protein IbpA. Asterisks label single protein molecules entering/exiting the nanopore. An open and closed protein signal could not be identified. Measurement was performed in 15 mM Tris, 150 mM NaCl, pH 7.5 applying -60 mV to the *trans* side and sampling at 10 kHz with a 2 kHz Bessel filter. For figure preparation, all traces were additionally filtered with a 100 Hz Gaussian filter. Protein and ligand were added to the *cis* side of the pore.

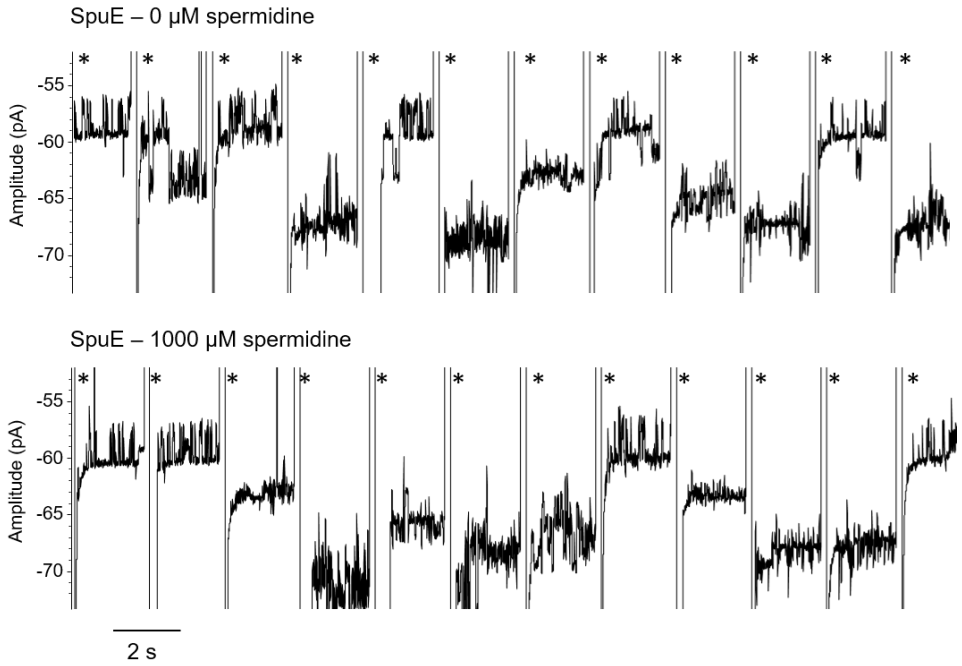

Figure S13. Protein blockades and binding curve of spermidine binding protein SpuE. Asterisks label single protein molecules entering/exiting the nanopore. An open and closed protein signal could not be identified. Measurement was performed in 15 mM Tris, 150 mM NaCl, pH 7.5 applying -70 mV to the *trans* side and sampling at 10 kHz with a 2 kHz Bessel filter. For figure preparation, all traces were additionally filtered with a 100 Hz Gaussian filter. Protein and ligand were added to the *cis* side of the pore.

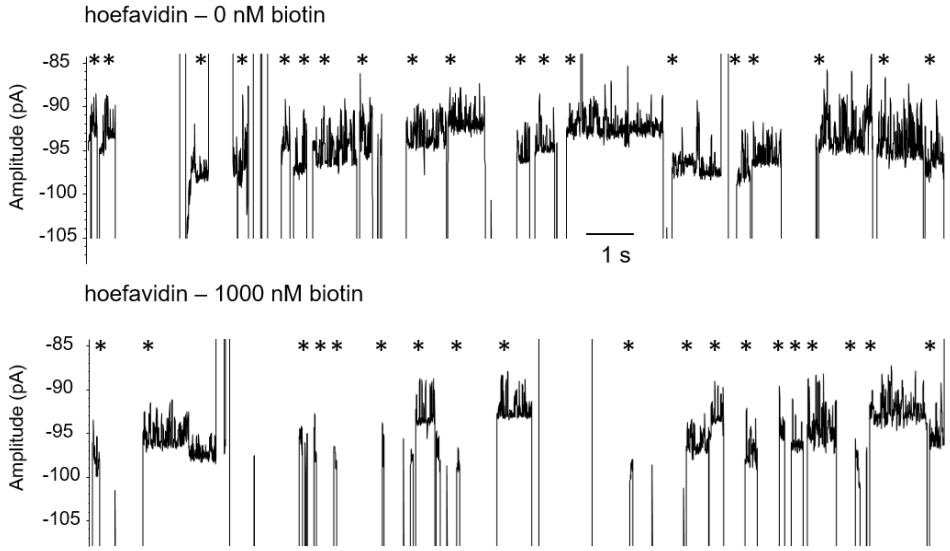

Figure S14. Protein blockades and binding curve of biotin binding protein hoefavidin (short version). Asterisks label single protein molecules entering/exiting the nanopore. An open and closed protein signal could not be identified. Measurement was performed in 15 mM Tris, 150 mM NaCl, pH 7.5 applying -90 mV to the *trans* side and sampling at 10 kHz with a 2 kHz Bessel filter. For figure preparation, all traces were additionally filtered with a 100 Hz Gaussian filter. Protein and ligand were added to the *cis* side of the pore.

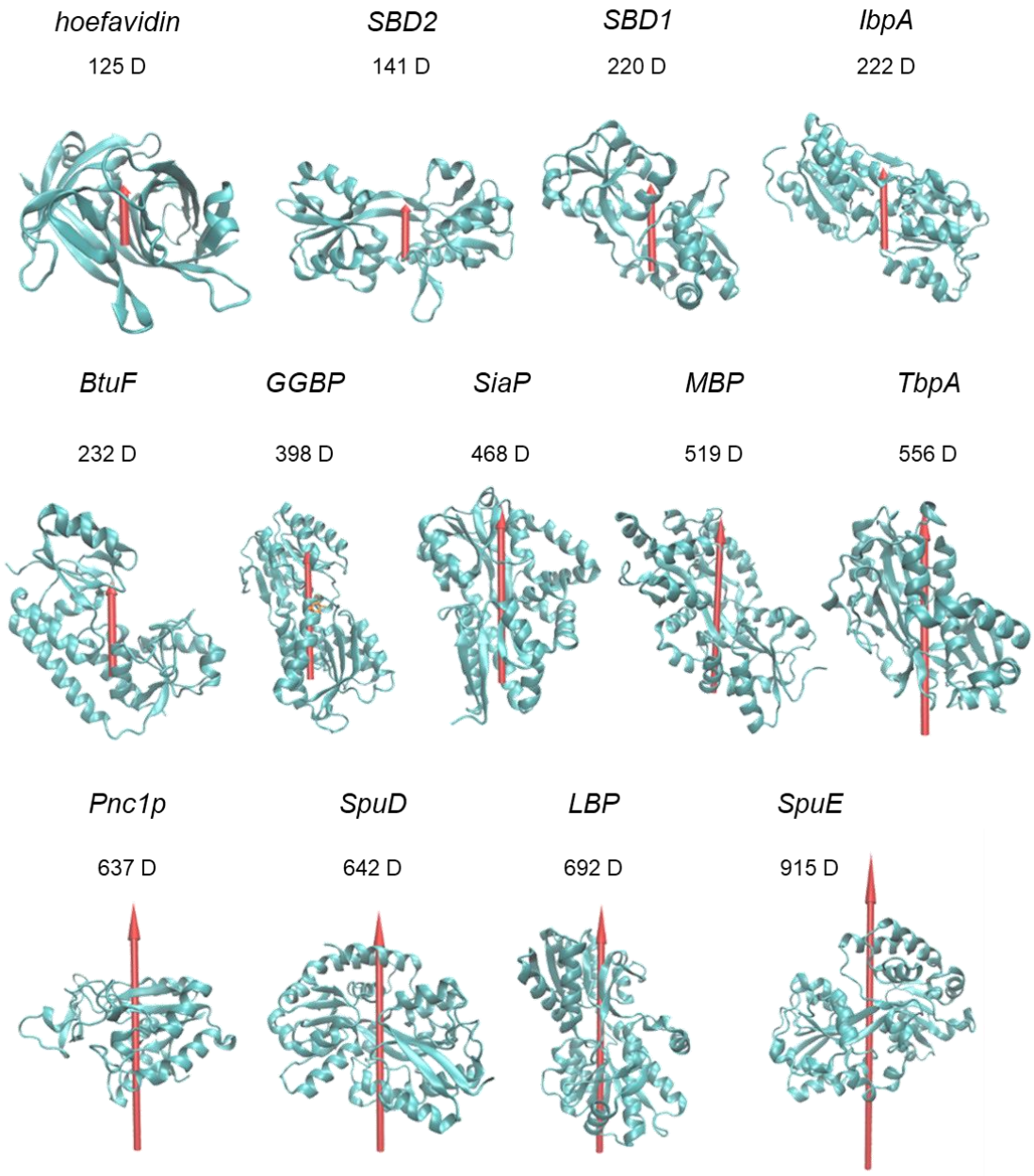

Figure S15. Dipole orientation and strength of the tested proteins. The dipoles were calculated and the figure prepared using with VMD.

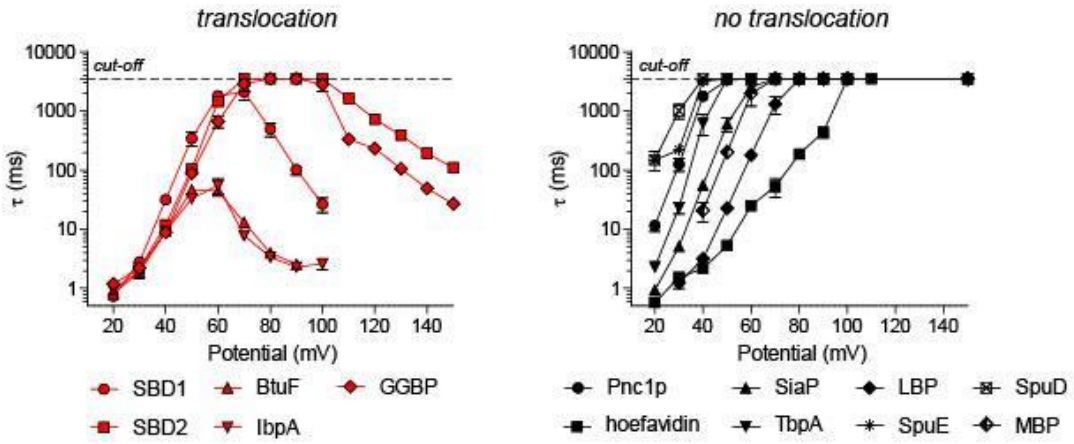

Figure S16. Translocation of proteins across ClyA. The dwell time was determined from at least 100 protein blockades. All experiments were performed in triplicates using 15 mM Tris, 150 mM NaCl, pH 7.5. TbpA Y27A and Pnc1p_dipole instead of the wild type proteins. All experiments were performed in triplicates. The error bars represent the standard error of the mean.